IEEE Access
Multidisciplinary | Rapid Review | Open Access Journal

IEEE ENGINEERING IN MEDICINE AND BIOLOGY SOCIETY SECTION

Received March 2, 2021, accepted April 20, 2021, date of publication May 4, 2021, date of current version May 14, 2021.

Digital Object Identifier 10.1109/ACCESS.2021.3077370

Fractal Analysis of MRI Data at 7 T: How Much Complex Is the Cerebral Cortex?

CHIARA MARZI[1], (Member, IEEE), MARCO GIANNELLI[2], CARLO TESSA[3], MARIO MASCALCHI[4], AND STEFANO DICIOTTI[1,5], (Senior Member, IEEE)

[1]Department of Electrical, Electronic, and Information Engineering "Guglielmo Marconi," University of Bologna, 47522 Cesena, Italy
[2]Unit of Medical Physics, Pisa University Hospital "Azienda Ospedaliero-Universitaria Pisana," 56126 Pisa, Italy
[3]Radiology Unit Apuane e Lunigiana, Azienda USL Toscana Nord Ovest, 54100 Massa, Italy
[4]Department of Experimental and Clinical Biomedical Sciences "Mario Serio," University of Florence, 50139 Florence, Italy
[5]Alma Mater Research Institute for Human-Centered Artificial Intelligence, University of Bologna, 40121 Bologna, Italy

Corresponding author: Stefano Diciotti (stefano.diciotti@unibo.it)

ABSTRACT The human brain is a highly complex structure, which can be only partially described by conventional metrics derived from magnetic resonance imaging (MRI), such as volume, cortical thickness, and gyrification index. In the last years, the fractal dimension (FD) – a useful quantitative index of fractal geometry – has proven to well express the morphological complexity of the cerebral cortex. However, this complexity is likely higher than that we can observe using MRI scanners with 1.5 T or 3 T field strength. Ultrahigh-field MRI (UHF-MRI) improves imaging of smaller anatomical brain structures by exploring down to a submillimetric spatial resolution with higher signal-to-noise and contrast-to-noise ratios. Accordingly, we hypothesized that UHF-MRI might reveal a higher level of the structural complexity of the cerebral cortex. In this study, using an improved box-counting algorithm, we estimated the FD of the cerebral cortex in six public or private T1-weighted MRI datasets of young healthy subjects (for a total of 87 subjects), acquired at different field strengths (1.5 T, 3 T, and 7 T). Our results showed, for the first time, that MRI-derived FD values of the cerebral cortex imaged at 7 T were significantly higher than those observed at lower field strengths. UHF-MRI provides an anatomical definition not achievable at lower field strengths and can improve unveiling the real structural complexity of the human brain.

INDEX TERMS Brain, cerebral cortex, complexity, fractal dimension, ultrahigh-field magnetic resonance imaging.

I. INTRODUCTION

The human brain is highly complex both in its structure and functions. This high level of complexity enables to efficiently control all the body functions and interpret information from the outside world. Magnetic resonance imaging (MRI) plays an increasingly important role in the *in vivo* non-invasive evaluation of the complexity of the brain and in particular of the cerebral cortex that is reflected in its highly ordered and intricated structure [1]. Neuroimaging biomarkers are important tools for understanding subtle morphological changes due to physiological brain maturation and healthy aging, as well as neurological diseases. However, conventional morphological metrics derived from MRI (e.g., volume, cortical thickness and gyrification index) can capture only partially the high structural complexity of the cerebral cortex.

The fractal geometry can describe the morphological complexity of objects that show *self-similarity*, geometrical or at least statistical, in a proper range of spatial scales [2], [3]. In particular, the most widely used index of fractal geometry, i.e., the fractal dimension (FD), has the potential to provide crucial and complementary information, while, at the same time, summarizes cortical thickness, sulcal depth, and folding area into a single numeric value [4]. In 1991, Hofman firstly showed that the whole cerebral cortex manifests fractal features [5]. Then, the fractal properties of the cerebral cortex have been widely investigated and FD has proven to be a valuable quantitative index of cortical complexity [4], [6]–[8]. Indeed, the FD was able to detect morphological subtle changes in healthy brain maturation [9], [10] and physiological aging [10]–[12], as well as to identify alterations in

The associate editor coordinating the review of this manuscript and approving it for publication was Alessandra Bertoldo.

the folding structure associated with abnormal brain development [13]–[15] and neurodegeneration [16]–[19].

Currently, the fractal analysis has consistently been applied on brain MRI at 1.5 and 3 T, which allows an exploration of the human brain typically down to 1 mm – the spatial scale equal to the size of the voxel of typical 3-D T1-weighted images. Thus, by this way, we can probe only a few of the spatial scales of observation in which the cerebral cortex might exhibit statistical self-similarity. Reasonably, the cerebral cortex is likely to exceed that we can explore with conventional 1.5 T and 3 T MRI scanners.

The not-quite-new but not-yet-fully-investigated ultrahigh-field (UHF) MRI, i.e., at 7 T, can lead to many advancements in the investigation of the morphological complexity of the brain. Indeed, the higher signal-to-noise-ratio (SNR), spatial resolution and contrast-to-noise-ratio (CNR) achievable at 7 T can allow higher sensitivity to tissue properties and anatomical details, resulting in clearer tissue boundaries [20].

The capability of imaging smaller anatomical structures and the possibility to explore more spatial scales (down to the typical submillimetric spatial resolution of UHF-MRI scanners) might allow an estimate of the FD of the cerebral cortex closer to its real (unknown) value. Notably, the fractal analysis has not been yet applied on brain images acquired at UHF-MRI.

For these reasons, in this study, we aimed at analyzing the fractal properties of the cerebral cortex in datasets of T1-weighted MR images acquired at various field strengths (1.5 T, 3 T and 7 T). In particular, we hypothesized that UHF-MRI has the potential to reveal a higher level of structural complexity of the cerebral cortex, in terms of FD, when compared to that measured using typical MRI acquisitions at 1.5 T or 3 T.

The manuscript is organized as follows. Section II describes the methodology in detail. In particular, in subsections II-A and II-B the datasets are introduced. In subsections II-C, II-D, II-E, and II-F the data processing and statistical analysis are described. Results are detailed in Section III and discussed in Section IV.

II. MATERIALS AND METHODS

In this study, we used six public or private datasets of T1-weighted MR images of healthy subjects acquired at various field strengths (1.5 T, 3 T and 7 T). In particular, four datasets have been used for a quantitative comparison among the FD estimates. Two other datasets containing T1-weighted images of the same subjects (one and two subjects, respectively) at different field strengths were used for a more qualitative analysis. The main characteristics of each dataset are summarized in Table 1 and detailed in the following subsections.

A. DATASETS FOR QUANTITATIVE GROUP ANALYSIS

From the datasets of subjects examined at 3 T and 1.5 T, we selected subjects in order to match age and sex with those belonging to the 7T dataset and, at the same time, to maximize the number of subjects selected (see next subsections and Table 1). The age- and sex-matching was performed after the tissue segmentation process (see subsection II-C), in order to consider only the subjects whose T1-weighted images were successfully processed. After this procedure, no significant differences were found among datasets for both age (p-value = 0.49 at ANOVA test) and sex (p-value = 0.17 at χ^2 test).

1) 7T DATASET

The 7T dataset included the T1-weighted images of healthy subjects belonging to the Consortium for reliability and reproducibility (CoRR) and publicly available at https://openneuro.org/datasets/ds001168/ [21]. This public dataset contains 22 participants (10 women), acquired on a 7 T whole-body MRI scanner (MAGNETOM 7 T, Siemens Healthcare, Erlangen, Germany) using a 3-D Magnetization Prepared two Rapid Gradient Echo (MP2RAGE) [22] sequence with an isotropic voxel size of 0.7 mm (further details in [21]). Due to segmentation errors (see subsection II-C), 5 subjects were excluded. Thus, in this study, 17 subjects were considered for further analysis (Table 1).

2) 3T_A DATASET

The 3T_A dataset was formed by 14 subjects out of 21 healthy volunteers belonging to the Kirby21 dataset [23], who were selected in order to match age and sex of those of the 7T dataset (Table 1). The data are part of the ''Multi-Modal MRI Reproducibility Resource'' (MMRR) and are accessible via the Neuroimaging Informatics Tools and Resources Clearinghouse (NITRC, http://www.nitrc.org/projects/multimodal). The T1-weighted images were acquired on a 3 T scanner (Achieva, Philips Medical System, Best, The Netherlands), using a high-resolution 3-D sequence (Magnetization Prepared Rapid Gradient Echo, MPRAGE) with a voxel size equal to 1 mm × 1 mm × 1.2 mm (further details in [23]).

3) 3T_B DATASET

The 3T_B dataset was constituted using public data collected by the International Consortium for Brain Mapping (ICBM) and belonging to the 1000 Functional Connectomes Project (accessible at http://fcon_1000.projects.nitrc.org/). In order to match age and gender with those of the 7T dataset, we selected 33 subjects (Table 1). All subjects had high-resolution T1-weighted images acquired on a 3 T scanner (GE Healthcare, Chicago, IL, US) with an isotropic voxel size of 1 mm (further details in [24]).

4) 1.5T DATASET

The 1.5T dataset included data of healthy subjects used in a previous study [17]. In order to match age and sex with those of the 7T dataset, we selected 20 of the 24 healthy subjects (Table 1). The MRI scans were acquired on a 1.5 T scanner (Intera, Philips Medical System, Best, The Netherlands), employing an isotropic voxel size equal to 1 mm (further details in [17]).

TABLE 1. Main characteristics of all datasets. No significant differences among 7T, 3T_A, 3T_B and 1.5T datasets were found for age (p-value = 0.49 at ANOVA test) and sex (p-value = 0.17 at χ^2 test).

	7T	3T_A	3T_B	1.5T	3T&7T	7T_UHR
Field strength (T)	7	3	3	1.5	3 and 7	7
Acquisition voxel size (mm x mm x mm)	0.7 × 0.7 × 0.7	1 × 1 × 1.2	1 × 1 × 1	1 × 1 × 1	1 × 1 × 1 (3 T) 0.7 × 0.7 × 0.7 (7 T)	0.25 × 0.25 × 0.25 0.5 × 0.5 × 0.5 1 × 1 × 1
Number of subjects (M/F)	17 (8/9)	14 (8/6)	33 (13/20)	20 (14/6)	2 (2/0)	1 (1/0)
Age (years)						
mean ± standard deviation	25.2 ± 2.4	26.6 ± 2.6	25.15 ± 5.44	6.4 ± 2.1	23.0 ± 1.4	born 1982
(min - max)	(22.0-30.0)	(22.0-30.0)	(19.0-35.0)	(22.0-29.2)	(22.0–24.0)	

F, female; M, male

B. DATASETS FOR QUALITATIVE ANALYSIS

We have used two additional datasets containing, respectively, two healthy subjects acquired both at 3 T and 7 T (3T&7T dataset) and one subject examined at 7 T with different native ultrahigh isotropic resolution (UHR) equal to 0.25 mm, 0.5 mm and 1 mm (7T_UHR dataset).

1) 3T&7T DATASET

This dataset was a subset of the MMRR resource and contains MRI data of two subjects (men, age 22 and 24 years), who were examined on both a 3 T (Achieva, Philips Medical System, Best, The Netherlands) and 7 T (Achieva, Philips Medical System, Best, The Netherlands) scanner. The T1-weighted MR images were acquired using a high-resolution 3-D sequence [MPRAGE and Turbo Field Echo (TFE), for 3 T and 7 T scanner, respectively], with an isotropic voxel dimension of 1 mm for the 3 T scanner and of 0.7 mm for the 7 T scanner (further details in [23]).

2) 7T_UHR DATASET

The 7T_UHR dataset contained the T1-weighted images of a single young healthy subject (male, born in 1982), examined on a 7 T scanner (Siemens Healthcare, Erlangen, Germany) [25]. This subject was scanned with a native isotropic voxel size of 1 mm, 0.5 mm and 0.25 mm (further details in [25]). In particular, to achieve an adequate SNR, eight T1-weighted volumes were acquired with the voxel size of 0.25 mm using prospective motion correction and, after inhomogeneity correction and reorientation to a common space, the volumes were averaged to increase SNR.

C. CORTICAL RECONSTRUCTION AND SEGMENTATION OF THE CEREBRAL CORTEX

An overview of the T1-weighted image processing is presented in Fig. 1.

Completely automated cortical reconstruction and volumetric segmentation of each subject's structural T1-weighted scan was performed by using the FreeSurfer suite version 6.0, which is well documented (see [26] for a review) and freely available (http://surfer.nmr.mgh.harvard.edu/). The stable version 6.0 introduced improvements for better segmentation and surface reconstruction of images acquired on 7 T

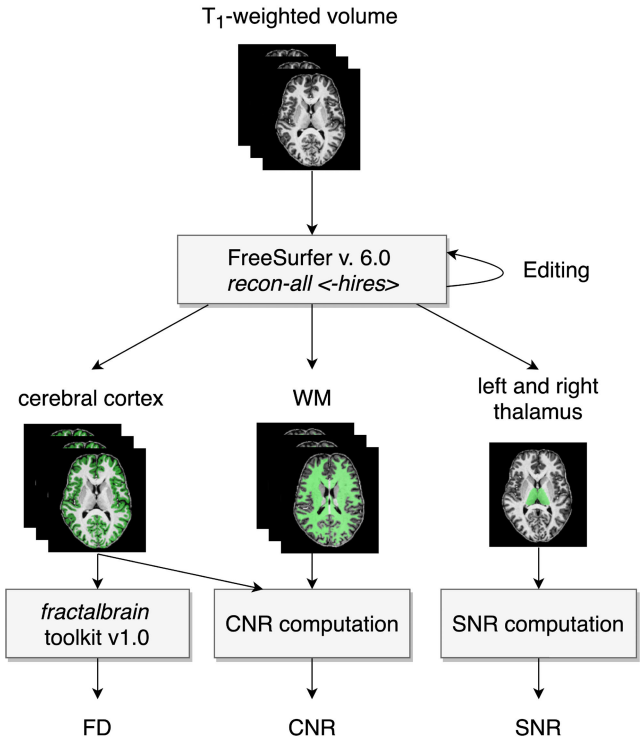

FIGURE 1. Overview of the processing applied on each T1-weighted scan (except for the 7T_UHR dataset, see text). CNR and SNR computation were performed in the datasets used for quantitative analysis. The *-hires* option has been used for all the images with voxel size smaller than 1 mm.

scanners. In particular, it allows to run the pipeline (*recon-all*) for data with voxel size less than 1 mm (*-hires* flag).

All the 1.5 T and 3 T T1-weighted images were processed at the default FreeSurfer isotropic voxel size (1 mm) using the standard *recon-all* pipeline. The data acquired at 7 T, with an isotropic voxel of 0.7 mm, were processed using the *-hires* flag in the *recon-all* procedure in order to preserve the submillimetric spatial resolution with the exception of the 7T_UHR dataset. Indeed, for the 7T_UHR dataset, we used the FreeSurfer version 5.3 outputs made available online by Lüsebrink *et al.* [25] (https://datadryad.org/stash/dataset/doi:10.5061/dryad.38s74). In particular, they downsampled each scan to

an isotropic resolution of 1 mm using the *recon-all* pipeline without the *-hires* flag.

Aiming to assess a possible effect on FD estimates of the voxel size selected during the T1-weighted images processing, we performed a further analysis. First, we upsampled the images of the 1.5 T dataset to an isotropic voxel size of 0.7 mm (1.5T_Upsampled dataset). Second, we downsampled the images of the 7 T dataset to an isotropic resolution of 1 mm (7T_Downsampled dataset). Both the upsampling and downsampling were carried out through a trilinear interpolation. The upsampled 1.5 T T1-weighted images were then segmented preserving the submillimetric spatial resolution, whereas the downsampled 7 T images were segmented using the standard *recon-all* procedure.

After the *recon-all* automated procedures, all the segmentations and surfaces reconstructions were visually inspected for defects and the correction methods proposed by the FreeSurfer developers were applied up to two times (http://surfer.nmr.mgh.harvard.edu/fswiki/FsTutorial/TroubleshootingData). The correction procedures consist of editing the brain mask and white matter (WM) mask (especially for the scans acquired at 7 T), adding control points and re-running the FreeSurfer pipeline. After all these procedures, in the CoRR dataset (at 7 T), the segmentation procedure failed for 5 subjects who were excluded, while the other subjects formed the 7T dataset (see II-A1 paragraph above). All segmentations of the other datasets were judged successful.

For the 7T, 3T_A, 3T_B, 1.5T and 3T&7T datasets, all the computations were performed on the same Dell PowerEdge T620 workstation equipped with two 8-core Intel Xeon E5-2640 v2, for a total of 32 CPU threads, and 128 GB RAM, using the Oracle Grid Engine batch-queuing system. The FreeSurfer segmentation and reconstruction procedure required ≈10 hours (with additional ≈5 hours for each re-running after manual correction) for each 1.5 T and 3 T scan, and ≈25-35 hours (with additional ≈17 hours for each re-running after manual correction) for each 7 T scan.

At the end of each FreeSurfer process, the 3-D binary mask of the cerebral cortex segmentation, obtained merging labels 3 (Left-Cerebral-Cortex) and 42 (Right-Cerebral-Cortex) of the aparc+aseg.mgz volume, entered the fractal analysis.

D. FRACTAL ANALYSIS

The FD of the cerebral cortex of each subject was estimated using the *fractalbrain* toolkit version 1.0 (freely available at https://github.com/chiaramarzi/fractalbrain-toolkit) [10]. *Fractalbrain* implements an improved box counting algorithm with automated selection of the fractal spatial scales. Briefly, let $I(x, y, z)$ be the 3-D binary segmentation of the cerebral cortex. Using the box counting algorithm [27], we superimpose on $I(x, y, z)$ a grid containing 3-D cubes of side s and we count the number of not null intersections between the grid and $I(x, y, z)$. This procedure is repeated for different s values, using an exponential sampling in the natural scale s (with $s = 2^k$ number of voxels, where $k = 0, 1, \ldots, 8$), which corresponds to a uniform sampling in the log-log plane. To reduce the bias introduced by the selection of a fixed grid origin, for each s value, we apply 20 uniformly distributed random offsets on the grid origin and we average all box counts (one for each offset) to obtain a single $N(s)$ value for each s [28]. Plotting $N(s)$ against s in a bi-logarithm plane, we fit a linear regression model and compute the FD as the slope (with the sign changed) of the regression line. In the natural scale, this linear relationship in the log-log plane corresponds to a power law $N(s) = K * s^{-FD}$, where FD is the exponent (with a negative sign) and K is the prefactor [3].

For an ideal fractal, the linear regression model can be theoretically fitted using a range of spatial scales starting from the object size down to an infinitesimal spatial scale. However, since the human brain is a real structure, it may exhibit fractal properties only over a narrower spatial range only and the actual assessment of this range is a fundamental prerequisite for a reliable and proper estimation of the FD of the cerebral cortex [29]. For this purpose, *fractalbrain* automatically selects the range of spatial scales where the cerebral cortex exhibits more marked fractal properties, identifying the range of s values in which the linear regression shows the highest coefficient of determination (adjusted for the number of data points) R^2_{adj}, and, in case of equal rounded R^2_{adj} coefficients, preferring the widest interval. Indeed, wide intervals are required for an object to be considered fractal [30]. This method has been proved to yield the most accurate machine learning models for individual age prediction as compared to other approaches in two international datasets of healthy subjects [10].

E. SNR AND CNR COMPUTATION

Theoretically, UHF-MRI at 7 T implies higher SNR values when compared with conventional MRI at 1.5 T or 3 T. This gain in SNR can be exploited – by properly setting the acquisition parameters – to improve the spatial resolution and the gray matter (GM)/WM CNR [31]–[33]. To characterize the image quality of different datasets, for each T1-weighted scan, we have estimated both the SNR and CNR.

For each T1-weighted scan data, a circular 2-D region of interest (ROI) was selected for SNR estimation. The ROI was automatically centered at the centroid of a reasonable homogeneous brain region. For this purpose, we chose the thalamus, previously segmented through FreeSurfer, in the axial slice in which the thalamus mask showed the largest area. We drew a circular ROI of about 1 cm in diameter (9 mm for images with a voxel size of 1 mm and 9.1 mm for scans with a voxel size of 0.7 mm), corresponding to the maximum possible value that allowed the ROI to be completely included within the segmentation mask of the thalamus. In this way, we ensured that all the pixels of the ROI were within the thalamus mask. Thus, the SNR was calculated as the mean signal intensity divided by the standard deviation within the ROI [33]. The SNR was measured on both the right and left

thalamus and the mean SNR was computed for each T1-weighted scan.

The CNR was estimated as the difference between the mean signal of WM and GM segmentations, divided by the standard deviation of the signal in the WM, as suggested by Springer *et al.* [33].

Both the SNR and CNR computations were implemented in Python language, using the neuroimaging package NiBabel 3.1.0 [34].

F. DATA ANALYSIS

1) DATASETS FOR QUANTITATIVE GROUP ANALYSIS

For each dataset (1.5T, 3T_A, 3T_B and 7T), we calculated the descriptive statistics of the FD values of the cerebral cortex along with those of SNR and CNR.

Then, we evaluated possible differences among datasets for FD, SNR and CNR values through the non-parametric Kruskal-Wallis test [35]. We computed post hoc Dunn's test, i.e., pairwise tests for multiple comparisons of mean rank sums [36] using the Bonferroni method for adjusting p-values. For each test, we considered an adjusted significance threshold of $\alpha = 0.05$.

To further investigate a possible association between FD values and the acquisition voxel size, potential differences in FD values between 1.5T_Upsampled vs. 7T and 1.5T vs. 7T_Downsampled datasets were evaluated through a non-parametric Mann-Whitney test. A significance threshold of $\alpha = 0.05$ was considered.

All statistical tests were performed in custom Python scripts using scipy v. 1.4.1, scikit_posthocs v. 0.6.4 and statsmodels v. 0.11.1 packages.

2) DATASETS FOR QUALITATIVE ANALYSIS

As previously mentioned, the 3T&7T and 7T_UHR datasets – collecting data of the same subjects acquired at different field strengths and/or at different native spatial resolutions – contained a too small number of subjects precluding any statistical analyses. For this reason, we applied only a qualitative data exploration to these datasets.

III. RESULTS

A. DATASETS FOR QUANTITATIVE GROUP ANALYSIS

The descriptive statistics of the FD of the cerebral cortex, SNR and CNR values are reported in Table 2.

TABLE 2. Descriptive statistics of the FD of the cerebral cortex, SNR and CNR of the 1.5T, 3T_A, 3T_B and 7T datasets. Median (interquartile range) values are reported.

	1.5T	3T_A	3T_B	7T
FD	2.4633 (0.0131)	2.4855 (0.0161)	2.5030 (0.0206)	2.5578 (0.0161)
SNR	15.58 (3.67)	20.20 (3.22)	20.84 (2.64)	15.86 (4.95)
CNR	3.32 (0.20)	2.66 (0.12)	3.40 (0.21)	4.87 (0.21)

TABLE 3. Post-hoc comparisons using Dunn's test of the FD of the cerebral cortex, SNR and CNR. Differences between median values (column - row) and post-hoc tests Bonferroni adjusted p-values are shown. * indicates median differences significant with a p-value < 0.05.

	1.5T	3T_A	3T_B	7T
		FD		
1.5T	0 (1.00)	0.03 (0.12)	0.04 (1.49e-5)*	0.1 (6.61e-14)*
3T_A		0 (1.00)	0.01 (0.61)	0.07 (8.98e-6)*
3T_B			0 (1.00)	0.06 (2.85e-4)*
7T				0 (1.00)
		SNR		
1.5T	0 (1.00)	4.62 (4.78e-3)*	5.26 (4.59e-8)*	0.28 (1.00)
3T_A		0 (1.00)	0.64 (0.85)	-4.34 (0.02)*
3T_B			0 (1.00)	-4.98 (2.05e-6)*
7T				0 (1.00)
		CNR		
1.5T	0 (1.00)	-0.66 (6.71e-3)*	0.08 (1.00)	1.55 (2.38e-6)*
3T_A		0 (1.00)	0.74 (1.18e-5)*	2.21 (4.31e-14)*
3T_B			0 (1.00)	1.47 (9.21e-5)*
7T				0 (1.00)

The FD, SNR and CNR median values differed significantly among datasets at the Kruskal-Wallis test (p-value $< 10^{-9}$) (Fig. 2). Post hoc pairwise comparisons for FD, SNR and CNR values are summarized in Table 3. In particular, the FD values of the cerebral cortex imaged at 7 T were significantly higher (post-hoc tests Bonferroni adjusted p-values $< 10^{-3}$ – see Table 3 for details) than those derived from images acquired at lower field strength (1.5 T and 3 T). Moreover, for all subjects, the lower limit of the range of spatial scale at 7 T was 0.7 mm. Finally, the FD of the cerebral cortex of the subjects belonging to the 1.5T dataset was smaller (post-hoc tests Bonferroni adjusted p-value $< 10^{-4}$) than those of subjects belonging to the 3T_B dataset (Fig. 2a).

The SNR values of the dataset acquired at 7 T showed significant smaller values than those observed at 3 T (post-hoc tests Bonferroni adjusted adjusted p-values < 0.05 – see Table 3 for details), while no significant difference between the SNR values of the 7T and 1.5T datasets was found. Also, the 1.5T dataset showed a SNR value significantly smaller than those of the datasets acquired at 3 T (post-hoc tests Bonferroni adjusted p-value < 0.01) (Fig. 2b).

Post-hoc pairwise tests revealed that T1-weighted images acquired at 7 T have higher CNR values as compared to scans acquired at 1.5 T and 3 T (post-hoc tests Bonferroni adjusted p-values $< 10^{-4}$ – see Table 3 for details). Moreover,

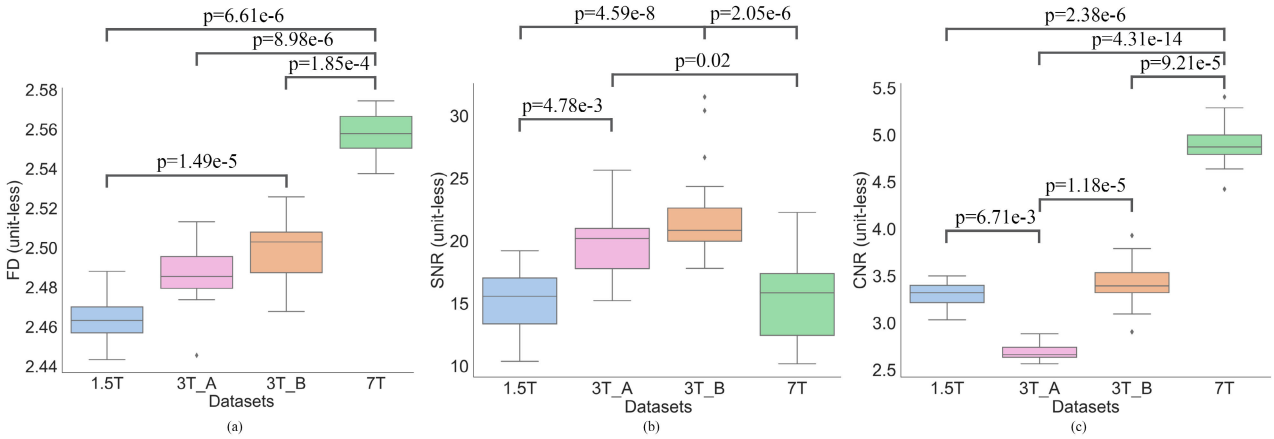

FIGURE 2. Box plot of the (a) FD of the cerebral cortex, (b) SNR and (c) CNR among 1.5T, 3T_A, 3T_B and 7T datasets. Post-hoc test Bonferroni adjusted p-values are reported when significant ($p<0.05$) (see Table 3 for details). The horizontal line inside each box represents the median value of the plotted data. The box shows the 1st and 3rd quartiles, while the whiskers extend to show the rest of the distribution, except for points that are determined to be outliers.

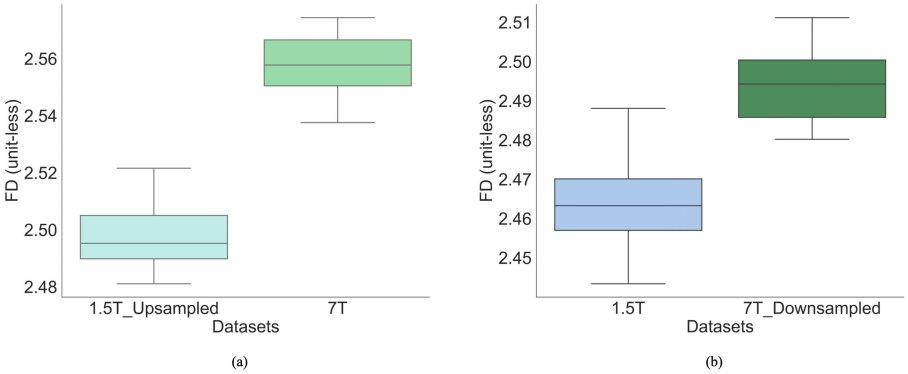

FIGURE 3. Box plot of the FD of the cerebral cortex for (a) 1.5T_Upsampled vs. 7T datasets and (b) 1.5T vs. 7T_Downsampled datasets. It is clearly noticeable that the FD of the cerebral cortex acquired natively at 7T is significantly higher as compared to that measured at 1.5T, irrespective of the resampling procedure [Mann-Whitney test p-values are $< 10^{-5}$ (see section III for details)]. The horizontal line inside each box represents the median value of the plotted data. The box shows the 1st and 3rd quartiles, while the whiskers extend to show the rest of the distribution, except for points that are determined to be outliers.

the dataset 3T_A showed the smallest median CNR value (Fig. 2c).

The median FD values of the images acquired at 1.5 T and upsampled to a voxel size of 0.7 mm [FD = 2.4953 (0.0152), median (interquartile range)] were still significantly lower than those of the images acquired at 7 T with a native resolution of 0.7 mm [FD = 2.5578 (0.0161)] (p-value $< 10^{-6}$ at Mann-Whitney test) (Fig. 3a). Moreover, the median FD values of the images acquired at 7 T and downsampled to a voxel size of 1 mm [FD = 2.4943 (0.0146)] were still significantly higher than those of the images acquired at 1.5 T with a native resolution of 1 mm [FD = 2.4633 (0.0131)] (p-value $< 10^{-5}$ at Mann-Whitney test) (Fig. 3b).

B. DATASETS FOR QUALITATIVE ANALYSIS

A preliminary data exploration carried out on the 3T&7T and 7T_UHR datasets showed a higher FD estimate at higher field strength and lower acquisition voxel size.

TABLE 4. FD values of the cerebral cortex of the subjects belonging to the 3T_7T dataset. The acquisition voxel size is also reported.

	3T	7T
	1 mm x 1 mm x 1 mm	0.7 mm x 0.7 mm x 0.7 mm
sub01	2.5001	2.5299
sub02	2.4909	2.5713

Indeed, the two subjects of the 3T&7T dataset, acquired both at 3 T (1 mm-native voxel size) and 7 T (0.7 mm-native resolution), yelded higher FD values at 7 T (Table 4). Moreover, for both subjects, the lower limit of the range of spatial scales at 7 T was 0.7 mm.

Finally, the 7T_UHR dataset, containing images of a single subject acquired on a 7 T scanner with a different native isotropic voxel size (i.e., 1 mm, 0.5 mm, and 0.25 mm) and resampled to a resolution of 1 mm, showed a gradual increase of FD of the cerebral cortex with decreasing the acquisition voxel size (see Table 5).

TABLE 5. FD values of the cerebral cortex of the subject belonging to the 7T_UHR dataset. The lenght of the acquisition voxel side is also reported.

	Isotropic voxel side 1 mm	Isotropic voxel side 0.5 mm	Isotropic voxel side 0.25 mm
subject	2.4785	2.4857	2.4894

IV. DISCUSSION

To our knowledge, this is the first study that has assessed the structural complexity of the cerebral cortex, in terms of FD, at 7 T. We found that UHF-MRI examinations were able to reveal a higher level of structural complexity of the cerebral cortex when compared to that observed at lower field strengths. These results seem to be directly related to the intrinsic properties of UHF-MRI acquisitions, and, in particular, to the higher CNR and improved spatial resolution. The SNR value of the 7 T dataset was not significantly different as compared to that of the 1.5 T dataset and was lower than those measured at 3 T. We can reasonably interpret this finding by considering that the differences in SNR values did not significantly impact the segmentation quality because all the scans in this study showed sufficient SNR to ensure a good quality segmentation.

The combination of the higher CNR and the smaller voxel size in acquisition could explain the ability of the UHF imaging to better resolve the structural complexity of the cerebral cortex. Indeed, in comparison to 1.5 T and 3 T, MRI at 7 T can result in a more accurate segmentation of brain tissues [20]. In particular, the higher CNR can help to distinguish WM, GM and CSF tissues [37]. Moreover, the higher spatial resolution allows a sharper definition of the WM/GM and GM/CSF interfaces. In this regard, we note that the spatial resolution in acquisition, rather than the voxel size in post-processing, is a key factor for a more accurate estimation of the structural complexity of the cerebral cortex. In fact, when imaged at 1.5 T with a native spatial resolution of 1 mm and resampled at 0.7 mm (1.5T_Upsampled dataset), the cerebral cortex still showed a lower FD as compared to the FD measured at 7 T with original spatial resolution of 0.7 mm (7T dataset). Similarly, downsampling the images acquired at 7 T with native spatial resolution of 0.7 mm to a spatial resolution of 1 mm (7T_Downsampled dataset), the FD values of the cerebral cortex remained higher than those computed at 1.5 T with native spatial resolution of 1 mm (1.5T dataset). This was confirmed also in the 7T_UHR dataset, in which the same subject was examined on a 7 T scanner at different native isotropic resolutions (0.25, 0.5 and 1 mm), and the FD of the cerebral cortex, resampled and segmented at the same spatial resolution of 1 mm, boosted when increasing the native spatial resolution (i.e., lower native voxel size).

Our results suggest that UHF-MRI has the potential to reveal more subtle changes in shape, showing a higher measure of complexity of the cerebral cortex. Our findings are in line with those by Chen and colleagues [38] who found an increase of the mean curvature (an alternative measure of structural complexity) of the right hemisphere when using 7 T data [38]. Other studies comparing conventional morphological metrics at different field strengths, including volumes [39], [40], cortical thickness, surface area and mean curvature [25], [38], [41], [42], reported that also these metrics varied across different field strengths and, in particular, the cortical thickness was overestimated by most studies at 3 T as compared to UHF examinations because of partial volume effects during the segmentation procedures [25], [38].

From a biophysical point of view, when the magnification level (i.e., spatial resolution) is increased, the morphology of the constituent elements, such as neurons, may become apparent [43] and the fractal properties may change or disappear. However, it is reasonable to hypothesize that this effect does not occur at the typical spatial resolution of T1-weighted MR images that is of approximately 1 mm. This was confirmed by the automated selection of the fractal spatial scales. Indeed, we found that the cerebral cortex still shows fractal properties at spatial scales down to 0.7 mm.

Our study has some limitations. First, we performed quantitative analyses on datasets which contained different samples of healthy subjects. Unfortunately, datasets composed of images acquired at various field strengths for the same subjects, which could be useful to confirm our findings, are actually very limited in the number of subjects. Second, the used different datasets we selected do not necessarily used the same acquisition sequence/parameters, which may be not optimal for estimating MRI-derived morphological metrics. However, we wish to point out that we used public or private MRI datasets acquisitions whose images parameters were those typically set in the current clinical and research routine without any a priori selection.

In conclusion, our results showed that MRI-derived FD values of the cerebral cortex at 7 T were significantly higher than those observed at lower field strengths. UHF-MRI allows improved anatomical definition of brain structures, with the potential of better unveiling the real structural complexity of the human brain.

REFERENCES

[1] V. Mountcastle, "The columnar organization of the neocortex," *Brain*, vol. 120, no. 4, pp. 701–722, Apr. 1997.
[2] B. Mandelbrot, "How long is the coast of Britain statistical self-similarity and fractional dimension," *Science*, vol. 156, no. 3775, pp. 636–638, May 1967.
[3] B. Mandelbrot, *The Fractal Geometry Nature*. San Francisco, CA, USA: Freeman, 1982. [Online]. Available: https://cds.cern.ch/record/98509
[4] K. Im, J.-M. Lee, U. Yoon, Y.-W. Shin, S. B. Hong, I. Y. Kim, J. S. Kwon, and S. I. Kim, "Fractal dimension in human cortical surface: Multiple regression analysis with cortical thickness, sulcal depth, and folding area," *Hum. Brain Mapping*, vol. 27, no. 12, pp. 994–1003, Dec. 2006.
[5] M. Hofman, "The fractal geometry of convoluted brains," *J Hirnforsch*, vol. 32, pp. 103–111, Oct. 1991.
[6] S. L. Free, S. M. Sisodiya, M. J. Cook, D. R. Fish, and S. D. Shorvon, "Three-dimensional fractal analysis of the white matter surface from magnetic resonance images of the human brain," *Cerebral Cortex*, vol. 6, no. 6, pp. 830–836, 1996. [Online]. Available: https://academic.oup.com/cercor/article-lookup/doi/10.1093/cercor/6.6.830
[7] V. G. Kiselev, K. R. Hahn, and D. P. Auer, "Is the brain cortex a fractal?" *NeuroImage*, vol. 20, no. 3, pp. 1765–1774, Nov. 2003. https://linkinghub.elsevier.com/retrieve/pii/S105381190300380X

[8] R. D. King, a. the Alzheimer's Disease Neuroimaging Initiative, A. T. George, T. Jeon, L. S. Hynan, T. S. Youn, D. N. Kennedy, and B. Dickerson, "Characterization of atrophic changes in the cerebral cortex using fractal dimensional analysis," *Brain Imag. Behav.*, vol. 3, no. 2, pp. 154–166, Jun. 2009. [Online]. Available: http://link.springer.com/10.1007/s11682-008-9057-9

[9] R. E. Blanton, J. G. Levitt, P. M. Thompson, K. L. Narr, L. Capetillo-Cunliffe, A. Nobel, J. D. Singerman, J. T. McCracken, and A. W. Toga, "Mapping cortical asymmetry and complexity patterns in normal children," *Psychiatry Res., Neuroimag.*, vol. 107, no. 1, pp. 29–43, Jul. 2001. [Online]. Available: https://linkinghub.elsevier.com/retrieve/pii/S0925492701000919

[10] C. Marzi, M. Giannelli, C. Tessa, M. Mascalchi, and S. Diciotti, "Toward a more reliable characterization of fractal properties of the cerebral cortex of healthy subjects during the lifespan," *Sci. Rep.*, vol. 10, no. 1, Dec. 2020, Art. no. 16957, [Online]. Available: http://www.nature.com/articles/s41598-020-73961-w

[11] C. R. Madan and E. A. Kensinger, "Cortical complexity as a measure of age-related brain atrophy," *NeuroImage*, vol. 134, pp. 617–629, Jul. 2016. [Online]. Available: https://linkinghub.elsevier.com/retrieve/pii/S1053811916300519

[12] C. R. Madan and E. A. Kensinger, "Predicting age from cortical structure across the lifespan," *Eur. J. Neurosci.*, vol. 47, no. 5, pp. 399–416, Mar. 2018. [Online]. Available: https://onlinelibrary.wiley.com/doi/abs/10.1111/ejn.13835

[13] Y.-T. Wu, K.-K. Shyu, T.-R. Chen, and W.-Y. Guo, "Using three-dimensional fractal dimension to analyze the complexity of fetal cortical surface from magnetic resonance images," *Nonlinear Dyn.*, vol. 58, no. 4, pp. 745–752, Dec. 2009. [Online]. Available: http://link.springer.com/10.1007/s11071-009-9515-y

[14] I. Nenadic, R. A. Yotter, H. Sauer, and C. Gaser, "Cortical surface complexity in frontal and temporal areas varies across subgroups of schizophrenia: Cortical surface complexity in schizophrenia subgroups," *Hum. Brain Mapping*, vol. 35, no. 4, pp. 1691–1699, Apr. 2014, [Online]. Available: http://doi.wiley.com/10.1002/hbm.22283

[15] K. L. Narr, R. M. Bilder, S. Kim, P. M. Thompson, P. Szeszko, D. Robinson, E. Luders, and A. W. Toga, "Abnormal gyral complexity in first-episode schizophrenia," *Biol. Psychiatry*, vol. 55, no. 8, pp. 859–867, Apr. 2004.

[16] C. Marzi, S. Ciulli, M. Giannelli, A. Ginestroni, C. Tessa, M. Mascalchi, and S. Diciotti, "Structural complexity of the cerebellum and cerebral cortex is reduced in spinocerebellar ataxia type 2: Structural complexity is reduced in SCA2," *J. Neuroimag.*, vol. 28, no. 6, pp. 688–693, Nov. 2018. [Online]. Available: http://doi.wiley.com/10.1111/jon.12534

[17] L. Pantoni, C. Marzi, A. Poggesi, A. Giorgio, N. De Stefano, M. Mascalchi, D. Inzitari, E. Salvadori, and S. Diciotti, "Fractal dimension of cerebral white matter: A consistent feature for prediction of the cognitive performance in patients with small vessel disease and mild cognitive impairment," *NeuroImage, Clin.*, vol. 24, 2019, Art. no. 101990. [Online]. Available: https://linkinghub.elsevier.com/retrieve/pii/S2213158219303407

[18] R. D. King, B. Brown, M. Hwang, T. Jeon, and A. T. George, "Fractal dimension analysis of the cortical ribbon in mild Alzheimer's disease," *NeuroImage*, vol. 53, no. 2, pp. 471–479, Nov. 2010. [Online]. Available: https://linkinghub.elsevier.com/retrieve/pii/S1053811910009080

[19] R. Sheelakumari, V. Rajagopalan, A. Chandran, T. Varghese, L. Zhang, G. H. Yue, P. S. Mathuranath, and C. Kesavadas, "Quantitative analysis of grey matter degeneration in FTD patients using fractal dimension analysis," *Brain Imag. Behav.*, vol. 12, no. 5, pp. 1221–1228, Oct. 2018. [Online]. Available: http://link.springer.com/10.1007/s11682-017-9784-x

[20] K. Bahrami, F. Shi, X. Zong, H. W. Shin, H. An, and D. Shen, "Reconstruction of 7T-like images from 3T MRI," *IEEE Trans. Med. Imag.*, vol. 35, no. 9, pp. 2085–2097, Sep. 2016. [Online]. Available: http://ieeexplore.ieee.org/document/7445872/

[21] K. J. Gorgolewski, N. Mendes, D. Wilfling, E. Wladimirow, C. J. Gauthier, T. Bonnen, F. J. M. Ruby, R. Trampel, P.-L. Bazin, R. Cozatl, J. Smallwood, and D. S. Margulies, "A high resolution 7-tesla resting-state fMRI test-retest dataset with cognitive and physiological measures," *Sci. Data*, vol. 2, no. 1, Dec. 2015, Art. no. 140054. [Online]. Available: http://www.nature.com/articles/sdata201454

[22] J. P. Marques, T. Kober, G. Krueger, W. van der Zwaag, P.-F. Van de Moortele, and R. Gruetter, "MP2RAGE, a self bias-field corrected sequence for improved segmentation and T1-mapping at high field," *NeuroImage*, vol. 49, no. 2, pp. 1271–1281, Jan. 2010. [Online]. Available: https://linkinghub.elsevier.com/retrieve/pii/S1053811909010738

[23] B. A. Landman, A. J. Huang, A. Gifford, D. S. Vikram, I. A. L. Lim, J. A. D. Farrell, J. A. Bogovic, J. Hua, M. Chen, S. Jarso, S. A. Smith, S. Joel, S. Mori, J. J. Pekar, P. B. Barker, J. L. Prince, and P. C. M. van Zijl, "Multi-parametric neuroimaging reproducibility: A 3-T resource study," *NeuroImage*, vol. 54, no. 4, pp. 2854–2866, Feb. 2011. [Online]. Available: https://linkinghub.elsevier.com/retrieve/pii/S1053811910015259

[24] J. Mazziotta *et al.*, "A probabilistic atlas and reference system for the human brain: International consortium for brain mapping (ICBM)," *Phil. Trans. Roy. Soc. London. Ser. B, Biol. Sci.*, vol. 356, no. 1412, pp. 1293–1322, Aug. 2001.

[25] F. Lüsebrink, A. Sciarra, H. Mattern, R. Yakupov, and O. Speck, "Erratum: T1-weighted *in vivo* human whole brain MRI dataset with an ultrahigh isotropic resolution of 250 μm," *Sci. Data*, vol. 4, no. 1, Dec. 2017, Art. no. 170032. [Online]. Available: http://www.nature.com/articles/sdata201732

[26] B. Fischl, "FreeSurfer," *NeuroImage*, vol. 62, no. 2, pp. 774–781, Aug. 2012. [Online]. Available: https://linkinghub.elsevier.com/retrieve/pii/S1053811912000389

[27] D. A. Russell, J. D. Hanson, and E. Ott, "Dimension of strange attractors," *Phys. Rev. Lett.*, vol. 45, no. 14, pp. 1175–1180, Oct. 1980.

[28] J. Goñi, O. Sporns, H. Cheng, M. Aznárez-Sanado, Y. Wang, S. Josa, G. Arrondo, V. P. Mathews, T. A. Hummer, W. G. Kronenberger, A. Avena-Koenigsberger, A. J. Saykin, and M. A. Pastor, "Robust estimation of fractal measures for characterizing the structural complexity of the human brain: Optimization and reproducibility," *NeuroImage*, vol. 83, pp. 646–657, Dec. 2013. [Online]. Available: https://linkinghub.elsevier.com/retrieve/pii/S1053811913007106

[29] G. A. Losa, "The fractal geometry of life," *Rivista di Biol.*, vol. 102, no. 1, pp. 29–59, 2009.

[30] F. Caserta, W. D. Eldred, E. Fernandez, R. E. Hausman, L. R. Stanford, S. V. Bulderev, S. Schwarzer, and H. E. Stanley, "Determination of fractal dimension of physiologically characterized neurons in two and three dimensions," *J. Neurosci. Methods*, vol. 56, no. 2, pp. 133–144, Feb. 1995. [Online]. Available: https://linkinghub.elsevier.com/retrieve/pii/016502709400115W

[31] S. Trattnig, W. Bogner, S. Gruber, P. Szomolanyi, V. Juras, S. Robinson, and S. Haneder, "Clinical applications at ultrahigh field (7 T). Where does it make the difference: Clinical applications at 7 T," *NMR Biomed.*, vol. 29, no. 9, pp. 1316–1334, Sep. 2016, [Online]. Available: http://doi.wiley.com/10.1002/nbm.3272

[32] S. Trattnig, E. Springer, W. Bogner, G. Hangel, B. Strasser, B. Dymerska, P. L. Cardoso, and S. D. Robinson, "Key clinical benefits of neuroimaging at 7 T," *NeuroImage*, vol. 168, pp. 477–489, Mar. 2018. [Online]. Available: https://linkinghub.elsevier.com/retrieve/pii/S1053811916306516

[33] E. Springer, B. Dymerska, P. L. Cardoso, S. D. Robinson, C. Weisstanner, R. Wiest, B. Schmitt, and S. Trattnig, "Comparison of routine brain imaging at 3 T and 7 T," *Investigative Radiol.*, vol. 51, no. 8, pp. 469–482, Aug. 2016. [Online]. Available: https://journals.lww.com/00004424-201608000-00001

[34] M. Brett. (Apr. 2020). *Nipy/Nibabel: 3.1.0*. [Online]. Available: https://doi.org/10.5281/zenodo.3757992

[35] W. H. Kruskal and W. A. Wallis, "Use of ranks in one-criterion variance analysis," *J. Amer. Stat. Assoc.*, vol. 47, no. 260, pp. 583–621, Dec. 1952.

[36] O. J. Dunn, "Multiple comparisons using rank sums," *Technometrics*, vol. 6, no. 3, pp. 241–252, Aug. 1964. [Online]. Available: http://www.tandfonline.com/doi/abs/10.1080/00401706.1964.10490181

[37] N. Zaretskaya, B. Fischl, M. Reuter, V. Renvall, and J. R. Polimeni, "Advantages of cortical surface reconstruction using submillimeter 7 T MEMPRAGE," *NeuroImage*, vol. 165, pp. 11–26, Jan. 2018. [Online]. Available: https://linkinghub.elsevier.com/retrieve/pii/S105381191730808X

[38] M. L. Z. Chen and L. MQ, "Morphometry of human brain: Intra-individual comparison between 3T and 7T high resolution structural mr imaging," *Chin. Med. Sci. J.*, vol. 32, no. 4, pp. 226–231, 2017.

[39] R. Heinen, W. H. Bouvy, A. M. Mendrik, M. A. Viergever, G. J. Biessels, and J. de Bresser, "Robustness of automated methods for brain volume measurements across different MRI field strengths," *PLoS ONE*, vol. 11, no. 10, Oct. 2016, Art. no. e0165719. [Online]. Available: https://dx.plos.org/10.1371/journal.pone.0165719

[40] J. Jovicich, S. Czanner, X. Han, D. Salat, A. van der Kouwe, B. Quinn, J. Pacheco, M. Albert, R. Killiany, and D. Blacker, "MRI-derived measurements of human subcortical, ventricular and intracranial brain volumes: Reliability effects of scan sessions, acquisition sequences, data analyses, scanner upgrade, scanner vendors and field strengths," *NeuroImage*, vol. 46, no. 1, pp. 177–192, May 2009. [Online]. Available: https://linkinghub.elsevier.com/retrieve/pii/S1053811909001505

[41] X. Han, J. Jovicich, D. Salat, A. van der Kouwe, B. Quinn, S. Czanner, E. Busa, J. Pacheco, M. Albert, R. Killiany, P. Maguire, D. Rosas, N. Makris, A. Dale, B. Dickerson, and B. Fischl, "Reliability of MRI-derived measurements of human cerebral cortical thickness: The effects of field strength, scanner upgrade and manufacturer," *NeuroImage*, vol. 32, no. 1, pp. 180–194, Aug. 2006. [Online]. Available: https://linkinghub.elsevier.com/retrieve/pii/S1053811906001601

[42] B. C. Dickerson, E. Fenstermacher, D. H. Salat, D. A. Wolk, R. P. Maguire, R. Desikan, J. Pacheco, B. T. Quinn, A. Van der Kouwe, D. N. Greve, D. Blacker, M. S. Albert, R. J. Killiany, and B. Fischl, "Detection of cortical thickness correlates of cognitive performance: Reliability across MRI scan sessions, scanners, and field strengths," *NeuroImage*, vol. 39, no. 1, pp. 10–18, Jan. 2008. [Online]. Available: https://linkinghub.elsevier.com/retrieve/pii/S1053811907007604

[43] G. Landini and J. P. Rigaut, "A method for estimating the dimension of asymptotic fractal sets," *Bioimaging*, vol. 5, no. 2, pp. 65–70, Jun. 1997. [Online]. Available: http://doi.wiley.com/10.1002/1361-6374%28199706%295%3A2%3C65%3A%3AAID-B%IO3%3E3.3.CO%3B2-5

CHIARA MARZI (Member, IEEE) was born in Reggio Emilia, Italy, in 1990. She received the B.S. and M.S. degrees *(cum laude)* in biomedical engineering and the Ph.D. degree in biomedical, electrical and systems engineering from the Alma Mater Studiorum University of Bologna, Italy, in 2016 and 2020, respectively.

Her research interest includes biomedical imaging. She is involved in research projects for the development and application of computational methods for the analysis of structural and functional MRI of the brain and the development of machine learning techniques for neuroimaging data. She received the "Alberto Mazzoldi" (University of Pisa) Award from the National Bioengineering Group for her Ph.D. thesis.

MARCO GIANNELLI received the master's degree from the Medical Physics School, University of Pisa, Pisa, Italy, in 2001.

Since 2002, he has been working with the Unit of Medical Physics–Pisa University Hospital, Italy. His research interest includes medical imaging. He worked on quality controls and characterization of scanners for quantitative MRI and computed tomography imaging. Moreover, his field of study is the application of quantitative MRI techniques in neurodegenerative disorders, breast cancer, and cardiac pathologies. Since 2002, he has also been a member of the Italian Association of Medical Physics (AIFM) and holds the national (Italy) qualification for an Associate Professor of Applied Physics, since 2013.

CARLO TESSA was born in Lucca, Italy, in 1965. He received the Laurea degree (Hons.) in medicine and the master's degree in radiology from the University of Pisa, Pisa, Italy, in 1991 and 1995, respectively, and the Ph.D. degree in neuroscience from the University of Florence, Florence, Italy, in 2004.

From 1997 to 2001, he was a Medical Specialist with the Radiology Unit, "Campo di Marte" Hospital, Lucca. From 2001 to 2020, he was also a Medical Specialist with the Radiology Unit, Versilia Hospital, Lido di Camaiore, Italy. Since November 2020, he has been the Director of the "Apuane e Lunigiana" Radiology Unit, Massa, Italy. His research interests include biomedical imaging, and in particular at MRI applied to neurodegenerative diseases and to cardiovascular diseases. He is also a member of the Società Italiana di Radiologia Medica (SIRM) and the European Society of Radiology (ESR).

MARIO MASCALCHI was born in Florence, Italy, in 1959. He received the Laurea degree (Hons.) in medicine from the Medical School, University of Florence, Florence, in 1984, the master's degree in neurology and the Ph.D. degree in applied physiopathology from the University of Florence, in 1988 and 1992, respectively, and the master's degree in radiology from the University of Florence, in 1996.

In 1998, he became a Researcher at the University of Florence, where, in 2001, he became an Associate Professor of Radiology. Since 2007, he has been a Full Professor of Translational Technical and Medical Sciences with the University of Florence. He is the author of 350 articles in refereed journals and his H index is 46. His current research interests include computed tomography of the lung and brain MRI.

STEFANO DICIOTTI (Senior Member, IEEE) was born in Florence, Italy, in 1975. He received the Laurea degree (Hons.) in electronic engineering from the University of Florence, Florence, in 2001, and the Ph.D. degree in bioengineering from the University of Bologna, Bologna, Italy, in 2005.

In 2013, he took the position of a Researcher at the University of Bologna, where, in 2019, he became an Associate Professor of Biomedical Engineering. He is currently with the Alma Mater Research Institute for Human-Centered Artificial Intelligence, Bologna. His current research interests include artificial intelligence for health and well-being and medical imaging. He is also a member of the IEEE Engineering in Medicine and Biology Society.